New observing modes of NACO

After more than two years of regular operation, a number of upgrades have recently been installed for NACO and offered to the community. The article describes the new observing modes and provides examples of astronomical applications in high-contrast imaging, spectroscopy and polarimetry.

Markus Kasper[1], Nancy Ageorges[2], Anthony Boccaletti[3], Wolfgang Brandner[4], Laird M. Close[6], Ric Davies[5], Gert Finger[1], Reinhard Genzel[5], Markus Hartung[2], Andreas Kaufer[2], Stephan Kellner[4], Norbert Hubin[1], Rainer Lenzen[4], Chris Lidman[2], Guy Monnet[1], Alan Moorwood[1], Thomas Ott[5], Pierre Riaud[3], Hermann-Josef Röser[4], Daniel Rouan[3], Jason Spyromilio[2]

[1]European Southern Observatory, Garching, Germany
[2]European Southern Observatory, Santiago, Chile
[3]LESIA, Observatoire de Paris, Meudon, France
[4]Max-Planck-Institut für Astronomie, Heidelberg, Germany
[5]Max-Planck-Institut für Extraterrestrische Physik, Garching, Germany
[6]Steward Observatory, Tucson, USA

NAOS-CONICA (hereafter NACO) is a near-infrared imager and spectrograph fed by an Adaptive Optics (AO) system to correct for optical aberrations introduced by atmospheric turbulence. NACO saw first light on November 25, 2001, at VLT UT4 (Brandner et al. 2002, Lagrange et al. 2003, Lenzen et al. 2003) and has been offered to the astronomical community since October 2002 (period 70). Since then, the science output of NACO amounts to more than 30 refereed articles with several highlights such as the confirmation of the black hole in the Galactic Centre (Schödel et al. 2002) and discovery of its flares (Genzel et al. 2003), as well as the dynamical calibration of the mass-luminosity relation at very low stellar masses and young ages (Close et al. 2005, see Figure 1).

The AO system NAOS was built by a French consortium comprised of Office National d'Etudes et Recherches Aérospatiales (ONERA), Observatoire de Paris and Laboratoire d'Astrophysique de l'Observatoire de Grenoble (LAOG). It compensates for the effects of atmospheric turbulence (seeing) and provides diffraction-limited resolution for observing wavelengths from 1 to 5 µm, resulting in a gain in spatial resolution by a factor of 5 to 15 (diffraction limit of an 8-m-class telescope in *K*-band corresponds to 60 mas). Active optical elements of NAOS include a tip-tilt plane mirror and a deformable mirror (DM) with 185 actuators. NAOS is equipped with two Shack-Hartmann type wavefront sensors (WFS) for wavefront sensing at optical (450 to 950 nm) and near-infrared (0.8 to 2.5 µm) wavelengths.

The near-infrared imager and spectrograph CONICA was built by the German Max-Planck-Institutes für Astronomie (MPIA) and für Extraterrestrische Physik (MPE) and ESO. In its original configuration, CONICA already provided six cameras for imaging and long-slit spectroscopy in the near-infrared between 1 µm and 5 µm at various spatial and spectral resolutions on a 1 × 1 kilopixel Aladdin detector, about 40 different filters for broad- and narrow-band imaging, Wollaston prisms and wiregrids for polarimetry, various grisms and a cryogenic Fabry-Perot interferometer for spectroscopy, as well as a Lyot-type coronagraph with different mask diameters.

The great flexibility of the instrument concept triggered many ideas on how the capabilities of NACO could be extended and optimized for certain specialized astronomical applications. For example, NACO was lacking a differential imaging mode and an adequate coronagraphic mode for high-contrast observations close to bright stars with the ultimate goal of detecting extrasolar planets. Both concepts are new developments for this kind of observations and have proven in theory to enhance the achievable contrast by orders of magnitude (Marois et al. 2000, Rouan et al. 2000). Additionally, new spectroscopic and polarimetric modes have been proposed with the main goal of increasing NACO's efficiency and minimize time overheads. Table 1 lists and briefly describes the recently offered modes and upgrades, of which the major ones will be discussed in the following sections of this article.

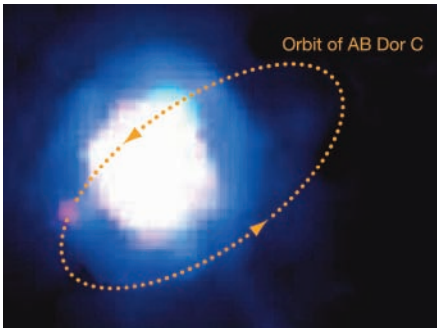

Figure 1: An enhanced false color infrared image of AB Dor A and C. The faint companion "AB Dor C" – seen as the pink dot at 8 o'clock – is 120 times fainter than its primary star. This is the faintest companion ever directly imaged within 0.156″ of its primary. Nevertheless, the new NACO SDI camera was able to distinguish it as a slightly "redder speckle" surrounded by the "bluer" speckles from AB Dor A. It takes 11.75 years for the 93 Jupiter mass companion to complete this orbit shown as a orange ellipse.

Upgrade	Date of installation	Offered since	Short description
SDI (simultaneous differential imager)	08/2003	P74	Uses a quad filter to take images simultaneously at 3 wavelengths surrounding the *H*-band methane feature at 1.62 μm. Performing a difference of images in these filters reduces speckle noise and helps to reveal faint methane companions next to bright stars.
4QPM (Four quadrant phase mask)	01/2004	P74	Subdivides the focal plane in quadrants and delays the light in two of them by half a wavelength at 2.15 μm. This coronagraphic technique helps to suppress the light of a star in order to reveal faint structures surrounding it.
Low-res prism	04/2004	P74	Allows for simultaneous spectroscopy from *J*- to *M*-band at R = 50 to 400.
Order sorting filters SL and SHK	04/2004	P74	Allows for *L*-band and *H*+*K*-band spectroscopy at various spectral resolutions.
Fabry-Perot interferometer	–	P74	Allows for narrow band (2 nm) observations tunable between 2 and 2.5 μm (for more information see Hartung et al. 2004).
Superachromatic retarder plate	04/2004	P75	Facilitates polarimetry by providing the possibility to rotate the position angle of polarization. Linear structure can thus be observed over the entire FoV and observation overheads are reduced.
New Aladdin III detector	05/2004	05/2004	Replaces old Aladdin II detector and has better cosmetics, linear range and read-noise.

Table 1: NACO upgrades

New Aladdin III detector

The most recent upgrade of NACO performed by the ESO IR department in collaboration with MPIA was the replacement of the CONICA Aladdin II detector. At larger reverse bias voltages (high dynamic range) the cosmetic properties of the old Aladdin II array were degraded substantially by a large number of warm pixels. For this reason, it was operated close to full well applying a low reverse bias voltage (for NACO users defined as high sensitivity mode) resulting in an acceptable cosmetic appearance. However, the charge storage capacity of the detector in this mode was small, and – as a property common to all infrared detectors operating in capacitive discharge mode – the response was quite nonlinear close to the full well capacity. The new Aladdin III array promised substantial improvements of the cosmetic properties.

After installation, the new detector behaved as expected and showed greatly improved cosmetic properties. In addition, it also showed lower read-noise and flux zero points which are lower by 0.1–0.4 magnitudes, suggesting a higher quantum efficiency of the new array as summarized in Table 2.

Simultaneous Differential Imager (SDI)

Radial velocity searches provide evidence that giant extrasolar planets are common. By September 2004, 136 extrasolar planets had been discovered and about 6% of the observed stars in the solar neighborhood host extrasolar planets (see *www.exoplanets.org*). However, the radial velocity method is most sensitive to planets in close orbit up to a few AU and cannot measure parameters other than the planet's orbit and mass with an uncertainty due to the unknown inclination of the orbit. Direct detection of extrasolar planets is required if we are to learn about the objects themselves. With direct detection we can analyze photons directly from the companions allowing us to measure L_{bol}, T_{eff}, Spectral Type, and other critical physical characteristics of these poorly understood objects.

Young (100 Myr old) and massive (couple of Jupiter masses to 12 Jupiter masses) extrasolar planets are 100000 times more self-luminous than old (5 Gyr) extra-solar planets, whereas their host stars are only slightly brighter when this young. The luminosity contrast between them can thus be in the range 10^{-4} to 10^{-6} with the precise value depending on age and mass of the planet. Currently the majority of such young stars that are nearby (< 50 pc) are located in the southern star forming regions and associations (DEC < –20). To detect a faint planet near a bright star requires the high Strehl ratios delivered by NACO. However, NACO (like all AO systems) suffers from a limiting "speckle-noise" floor which prevents the detection of planets within 1″ of the primary star. Hence NACO required some method to suppress this limiting "speckle noise" floor, so planets could be imaged within 1″ of their primary star.

The SDI concept to reduce speckle noise by L. M. Close from Steward Observatory and R. Lenzen from MPIA (Lenzen et al. 2004) is based on a method presented by Marois et al. (2000). This method exploits the fact that all extra-solar giant planets cooler than about 1300 K have strong CH_4 (methane) absorption past 1.62 μm in the *H*-band NIR atmospheric window, making the planet virtually disappear at this wavelength. The difference of two images taken simultaneously on either side of the CH_4 absorption therefore efficiently removes star and speckle noise while the planet remains. A critical point of the design is the differential optical aberration after the two wavelengths have been optically separated. It has to be kept very small (< 10 nm rms) in order to match the speckle pattern at the two wavelengths and efficiently remove it by the image subtraction.

Figure 2 shows the optical concept of SDI. A double Wollaston prism, made of two identical Calcite Wollaston prisms rotated against each other by 45 deg, splits the beam into four beams of equal brightness (for unpolarized objects). The f/40 camera images the four beams onto the detector with a minimum separation of 320 pixels or 5.5″ at the pixelscale of 17.2 mas per pixel. Currently, the field of view is limited by a field mask and the usable detector area to about 3″ × 3.7″. Just in front of the detector, each of the beams passes through one of a set of narrow band filters with central wavelengths of 1.575, 1.600 and 1.625 μm and a FWHM of 25 nm.

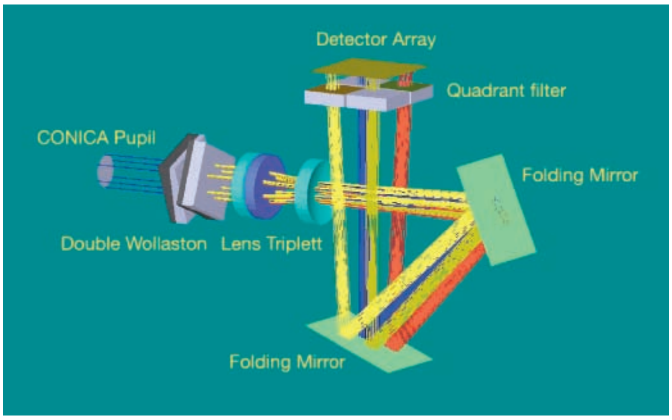

Figure 2: SDI optical concept. A double Wollaston prism splits the beam into four which are imaged through different filters located on the either side of the *H*-band methane feature at 1.62 μm.

	Pixels with variable dark current [%]			Readout noise [ADU]		Zero Points [mag]		
	High sensitivity	High dynamics	High well depth	Uncorr	Fowler	J	H	Ks
Aladdin II	0.72	7.1	56	5.6	2.1	24.01	23.87	22.99
Aladdin III	0.023	0.156	2.43	4.42	1.29	24.47	24.22	23.31

Table 2: Main properties of the old (Aladdin II) and the new (Aladdin III) Conica arrays.

The f/40 imaging optics was built such that it could just replace the existing camera L100 which had never been offered.

The contrast ratio achievable by SDI is more than two magnitudes better than that achieved by standard imaging and PSF subtraction using a subsequently observed point source. Figure 3 shows the achievable contrast for 5 sigma detection as a function of angular separation for a 32 minute exposure. The highest contrast (“double filtered”) is achieved by subtracting the images taken at two different rotator angles in addition to the dual image subtraction in order to reduce the remaining instrumental speckles and by filtering out the low spatial frequencies of the images. SDI removes most of the speckle noise such that the contrast is mostly limited by stellar photon noise at intermediate angular separations and by sky background and detector read-out noise at larger angular separations. In both cases, the achievable contrast can be further improved by increasing the integration time. Figure 4 shows a reduced double filtered SDI image. Companions 9.5 magnitudes fainter than the star, are easily detected outwards of 0.5″.

Although mainly conceived for exoplanet imaging, SDI is also very useful for observations of objects with thick atmospheres in the solar system like Titan. Peering at the same time through a narrow, unobscured near-infrared spectral window in the dense methane atmosphere and an adjacent non-transparent waveband, Figure 5 shows Titan’s surface regions with very different reflectivity in unprecedented detail when compared to other ground-based observations.

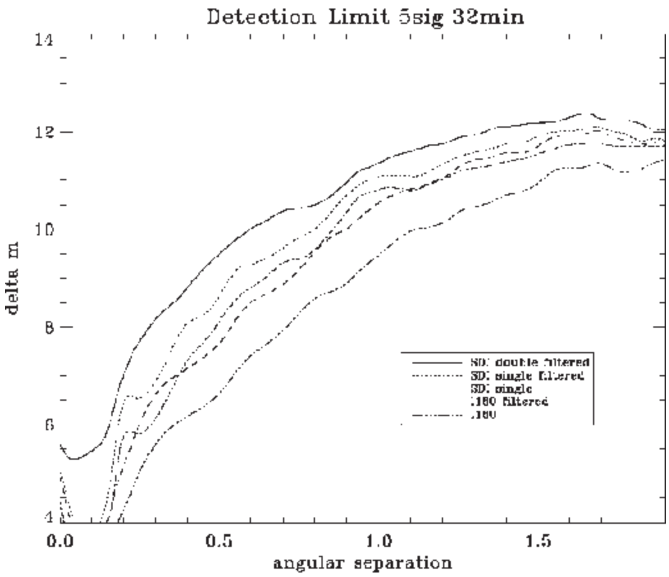

Figure 3: SDI detectivity as a function of angular separation from the star using different data reduction schemes. ‘SDI double filtered’ is a technique where the instrument is ro-tated half way through the observation to calibrate instrumental speckles with subsequent filtering of low spatial frequency structures. ‘I160’ denotes conventional imaging without speckle removal.

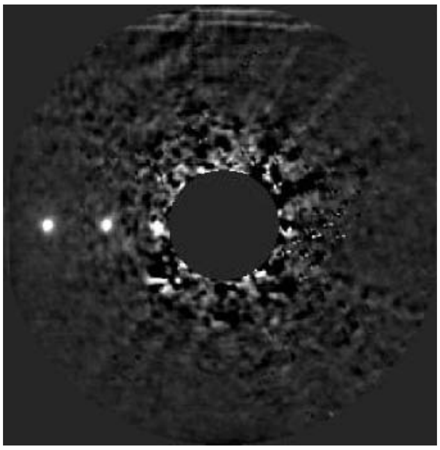

3.4″

Figure 4: Final SDI image (double filtered) derived from real data which was used to derive the detection limits shown in Figure 3. The three artificial companions at 0.5″, 1″ and 1.5″ with Δmag = 9.5 (5σ detection at 0.5″) are clearly visible.

Four-quadrant phase mask (4QPM)

As for the SDI, the main scientific motivation for the 4QPM coronagraph is to increase the contrast of faint objects around bright stars. Besides the search for faint point sources as described in the previous section, the 4QPM can be used to look for hot dust around AGN (see e.g. Gratadour et al. 2005), quasar host galaxies or circumstellar emission produced by disks very close (0.1″ to 0.5″) to the central point source.

The four quadrant phase-mask coronagraph was proposed by Rouan et al. (2000). The focal plane is split into four equal areas, two of which are phase-shifted by π. As a consequence, a destructive interference occurs in the relayed pupil, and the on-axis starlight transferred outside the geometric pupil is blocked by a so-called Lyot stop. The advantage of the 4QPM over the Lyot mask is twofold: (1) no large opaque area at the centre and an inner working radius of about

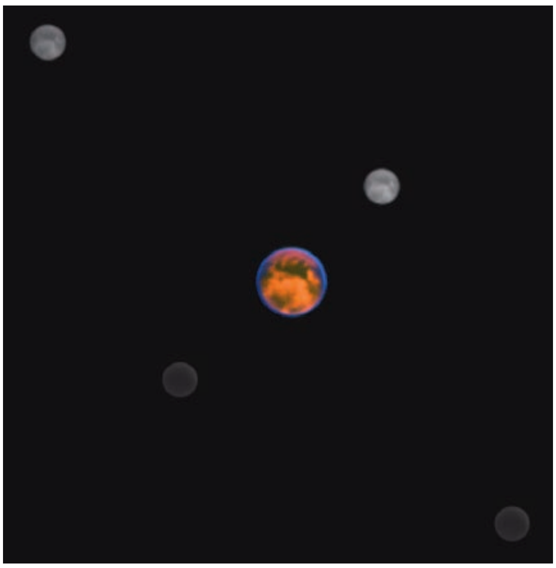

Figure 5: Titan imaged with SDI. The picture shows Titan imaged through the 4 channels of the SDI camera. Obviously, Titan appears very faint and featureless when imaged inside the methane band in the barely visible lower two images. The central color image is the difference between the out- and in-band images and has been added to the picture afterwards.

1 Airy disc, and (2) a larger achievable contrast if good optical quality is met.

The actual concept of the 4QPM in NACO as proposed by LESIA, Observatoire de Meudon, consists of a SiO_2 substrate with a 2.5 µm thick SiO_2 layer deposited on two of the quadrants. This device is placed in the CONICA mask wheel and has a working wavelength of 2.15 µm where it achieves the π phase-shift and maximum light rejection. The theoretically achievable PSF attenuation deteriorates with the square of the wavelength deviation from optimum. In practice, residual wavefront errors dominate over chromatic effects, and PSF core attenuation of about a factor 10 can be achieved all over the *K*-band while it drops to a modest factor of 4 in *H*-band (Boccaletti et al. 2004). Figure 6 displays the radial point source sensitivity achieved with NACO in a 10 minutes exposure observing a bright star. The actually achievable 4QPM performance and the contrast improvement by subtracting a subsequently observed reference PSF star strongly depend on the quality and stability of the AO correction.

Figure 7 (top) shows a beautiful example of an astronomical application of the 4QPM published by Gratadour et al.(2005). The observations show a complex environment closer to the nucleus than previously imaged at this wavelength. The identified structures are similar to what has been observed previously at longer wavelengths (3.8 and 4.8 µm), similar resolution, but without coronographic mask. Up to now they were totally hidden by the dominating emission of the nucleus at *Ks*. Shape and photometry are in very good agreement with the previous interpretation of elongated knots, shaped by the passage of a jet, and composed of very small dust grains, transiently heated by the central engine of the AGN. On the bottom of the figure, the image of a triple system HIP 1306 demonstrates the enhanced contrast for close companion detection achievable with the 4QPM.

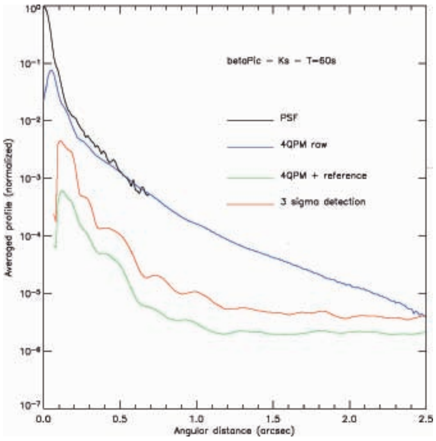

Figure 6: Radial detectivity of the 4QPM. The achievable 3σ detectivity is 10^{-4} (10 mag) at 0.5″ and 10^{-5} (12.5 mag) at 1″. Stellar residuals, i.e., the quality of the PSF reference subtraction, dominate at short angular distance, while sky and detector noise dominate at larger angular separations for this star magnitude and exposure time (courtesy Anthony Boccaletti).

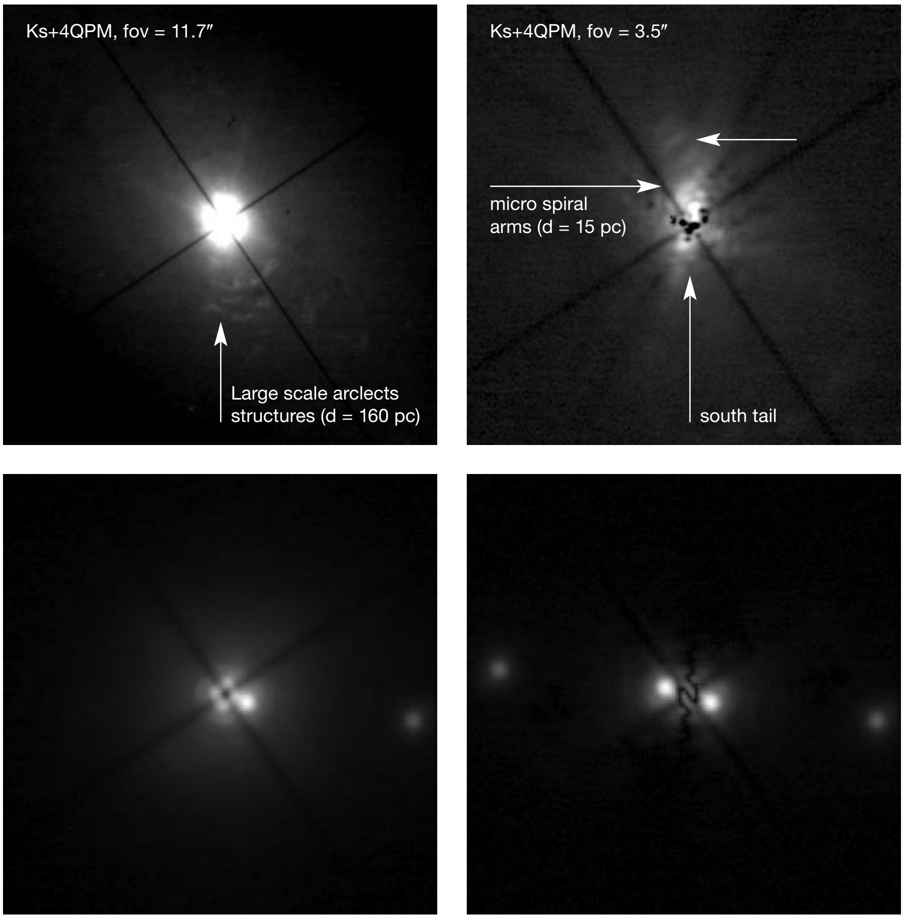

Figure 7: Top: Structures around NGC 1068 revealed at both large and close separations. The image to the right is PSF reference star subtracted. The contrast of known structures is improved with respect to previous non-coronagraphic observations (Gratadour et al. 2005). Bottom: Triple system imaged with the 4QPM. The two companions are at separations of 0.128″ and 1.075″ with brightness ratios to the main surpressed primary of Δm = 1.6 and 3.5 mag (Boccaletti et al. 2004).

Low-resolution prism

There are a number of research projects in which simultaneous, moderate resolution spectro-photometry would be useful and, in some cases, essential. Perhaps the most pressing and important case presently is the exploration of the infrared flares from the Galactic Centre black hole discovered with NACO. The flares promise to be a key tool for studying the physical processes in the strong gravity regime just outside the event horizon. For a better understanding of the emission mechanisms, it is necessary to obtain simultaneous spectral energy distributions (SED) across the *H*-through *L/M*-bands. Since the flares last typically only one hour and have time substructure of 10–20 minutes, it is not possible to obtain the data sequentially. Subtle time variability of the SED, as expected if gas falls in through the innermost accretion zone and experiences increasing gravitational redshift, also calls for simultaneous information. Other fields where the proposed new mode would be extremely useful are determination of stellar types in dense star clusters, dust features in AGN environments and spectral characterization of brown dwarfs with deep and characteristic broad atmospheric IR features.

The concept of the low spectral resolution mode of NACO has been developed by R. Lenzen from MPIA. $SrTiO_3$/CsBr turned out to be the best combination of a high dispersion and a low dispersion material, providing high transmission and a rather constant dispersion for the whole wavelength region. Figure 8 shows the spectral resolution achievable with different material combinations over the spectral range of the CONICA detector.

The low resolution prism was used by the Galactic Centre Group of the Max-Planck-Institut für Extraterrestrische Physik in July 2004 with the aim of measuring the spectral slope of the flaring source at SgrA* in the Galactic Centre. Since no flare was seen during this run, spectra of several stars in the central cluster were obtained instead, as a feasibility test and to better characterise the performance of the prism. The adaptive optics loop was closed on the infrared-bright IRS 7, using the infrared wavefront sensor. Due to the high extinction towards the Galactic Centre (A_V = 30 mag), there is little to be seen shortward of *H*-band; and because the *JHK* dichroic was used for the infrared wavefront sensor (in order to be able to detect the *LM*-bands) a 2.5 µm short cutoff filter was inserted. The resulting normalized *LM*-band spectra of 3 stars are shown in Figure 9 (IRS 7 with *K* ~ 6.7, IRS 16 NW with *K* ~ 9.5, and IRS 33 N with *K* ~ 10.5). Wavelength calibration was rather tricky and eventually achieved via a combination of narrow-band filter images and matching atmospheric absorption features. No correction for extinction has been applied to these spectra. Seeing limited *L*-band spectra of several other Galactic Centre stars have previously been published by Moultaka et al. (2004), and similar features can be clearly identified: H_2O ice absorption at 3.0 µm; CH_2 and CH_3 absorption at 3.4 µm; Pf γ and Brα emission at 3.74 µm and 4.05 µm respectively. The *M*-band data are the first such spectra of these Galactic Centre stars. The extraction of a spectrum for at least one of the S-sources (not shown) indicates that it should certainly be possible to obtain a 3–5.5 µm spectrum of a flare from SgrA* if one should be lucky enough to be using the prism at the right time. Actually, a *K*-band spectrum of a Galactic centre flare was obtained in July 2004 with the adaptive optics based 3D IR spectrometer SINFONI during its first commissioning run.

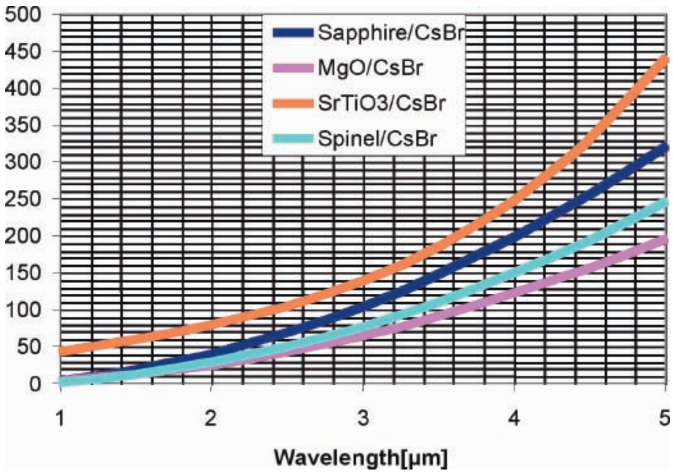

Figure 8: Spectral resolving power over the CONICA NIR range provided by prisms of different composition.

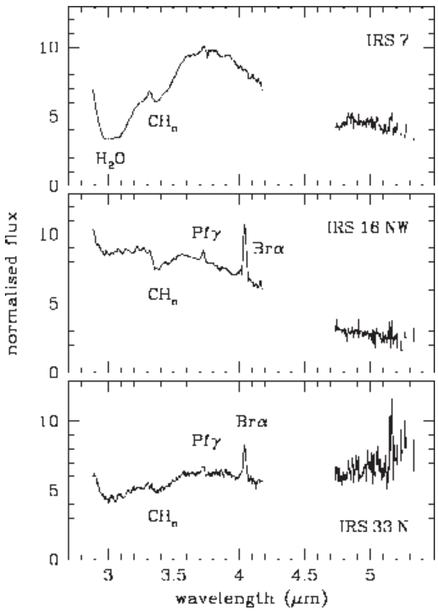

Figure 9 (left): *LM*-band spectra of IRS 7 with *K* ~ 6.7, IRS 16 NW with *K* ~ 9.5, and IRS 33 N with *K* ~ 10.5 obtained with the new low resolution prism.

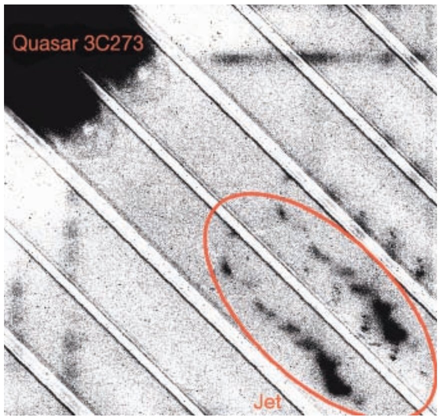

Figure 10 (below): Polarization data of the quasar 3C273 jet. NACO has been rotated to align the jet with the Wollaston stripe mask. The retarder plate can be used to turn the polarization direction in order to derive the polarization map (image prepared by Sebastian Jester).

Superachromatic retarder plate

For the detailed study of extragalactic radio jets NACO is a unique instrument. Especially in its polarization mode, information can be collected which can be combined with radio data at the same resolution in order to gain insight into the physics of these objects. Polarization studies in dusty star forming regions, circumstellar discs and envelopes, and scattering regions in AGN are other central areas where NACO is unparalleled.

Before the upgrade, polarimetry was possible using two Wollaston prisms with position angles 0° and 45° with two main limitations: (1) Linear structures (like a jet) could not be covered at once over their entire length, if these objects were longer than the angular separation of the Wollastons (3.3″). Then multiple images were necessary to cover the object completely, as by rotation to e.g. 45°, part of the object will fall out of the stripe mask. (2) With each rotation of the instrument between 0° and 45° a new alignment of the telescope pointing was necessary, leading to a substantial overhead in polarization observations.

With the new turnable retarder plate at the instrument entrance, just one Wollaston prism is used, and rotation of the plane of polarization is done by turning the plate. The retarder plate was put in place of the never offered TADC-device and is located about 12 cm pre-focal within the converging f/15 beam. The resulting focus shift due to the achromatic plate thickness of about 8 mm (3.43 mm MgF_2 thickness, 4.35 mm Quartz plate thickness) can be compensated by focus offsetting NAOS.

Figure 10 shows an example of polarimetry with NACO using one Wollaston prism and the retarder plate. The scientific goal of the observations was a polarization map of the jet of the quasar 3C273. The jet extends out to about 20″ from the quasar core located in the upper left. For this image, 94 exposures of 100 seconds each (NDIT = 1) have been added up. Only the common area of the field is shown. The jet does seem to exhibit a polarization signal (most conspicuous at inner and outer knots). Because the quasar is so bright, the image also reveals reflections due to the half wave plate and electronic ghosts within the detector.

Outlook

Although no further additional observing modes are planned so far, the work on NACO has not yet finished. The next major improvement of the system will be the installation of the Laser Guide Star Facility planned for spring/summer 2005. Additional components that NACO requires to operate with an LGS such as an additional STRAP tip tilt sensor as well as the necessary software upgrades have already been installed and tested. The first commissioning of NACO with the LGS is foreseen for fall/winter 2005. Then, a much larger fraction of astronomical objects will be accessible to the superb observing modes offered by NACO.

References

Boccaletti, A. et al. 2004, PASP, 116, 1061
Brandner, W. et al 2002, The Messenger, 107, 1
Close, L. M. et al. 2005, Nature, 433, 286
Genzel, R. et al. 2003, Nature, 425, 934
Gratadour, D. et al. 2005, A&A, 429, 433
Hartung, M. et al. 2004, Proc. SPIE, 5492, 1531
Hartung, M. et al. 2004, A&A, 421, L17
Lagrange, A. M. et al. 2003, Proc. SPIE, 4841, 860
Lenzen, R. et al. 2003, Proc. SPIE, 4841, 944
Lenzen, R. et al. 2004, Proc. SPIE, 5492, 970
Marois, C. et al. 2000, PASP, 112, 91
Moultaka, J. et al. 2004, A&A, 425, 529
Rouan, D. et al. 2000, PASP, 112, 1479
Schödel, R. et al. 2002, Nature, 419, 694